Geochemistry, Geophysics, Geosystems

RESEARCH ARTICLE
10.1029/2024GC011688

Key Points:

- The effects of varying lithosphere structure during supercontinent assembly can be observed in the mantle through the supercontinent cycle
- Thick, viscous continents promote steeper slab dips which can impact the proximity of slabs and plumes beneath a supercontinent interior
- Proximity of slabs to upwellings in the mantle may impact the magnitude of the plume and the extent of lithosphere thinning near the surface

Supporting Information:

Supporting Information may be found in the online version of this article.

Correspondence to:
A. Plimmer,
plimmerar@cardiff.ac.uk

Citation:
Plimmer, A., Davies, J. H., & Panton, J. (2024). Investigating the effect of lithosphere thickness and viscosity on mantle dynamics throughout the supercontinent cycle. *Geochemistry, Geophysics, Geosystems*, *25*, e2024GC011688. https://doi.org/10.1029/2024GC011688

Received 23 MAY 2024
Accepted 23 OCT 2024

Author Contributions:
Conceptualization: A. Plimmer, J. H. Davies
Data curation: A. Plimmer, J. H. Davies, J. Panton
Formal analysis: A. Plimmer
Funding acquisition: J. H. Davies
Investigation: A. Plimmer
Methodology: A. Plimmer
Project administration: A. Plimmer, J. H. Davies
Resources: J. H. Davies
Software: A. Plimmer, J. H. Davies
Supervision: J. H. Davies, J. Panton

Investigating the Effect of Lithosphere Thickness and Viscosity on Mantle Dynamics Throughout the Supercontinent Cycle

A. Plimmer[1], J. H. Davies[1], and J. Panton[1]

[1]School of Earth and Environmental Sciences, Cardiff University, Cardiff, UK

Abstract The relationship between the lithosphere and the mantle during the supercontinent cycle is complex and poorly constrained. The processes which drive dispersal are often simplified to two end members: slab pull and plume push. We aim to explore how lithosphere thickness and viscosity during supercontinent assembly may affect the interaction of deep mantle structures throughout the supercontinent cycle. We consider supercontinental lithosphere structure as one of many potential processes which may affect the evolution of upwellings and downwellings and therefore systematically vary the properties of continental and cratonic lithosphere, respectively within our 3D spherical simulations. The viscosity and thickness of the lithosphere alters the dip and trajectory of downwelling material beneath the supercontinent as it assembles. Focusing on Pangea, we observe that plumes evolve and are swept beneath the center of the supercontinent by circum-continental subduction. The proximity of these upwelling and downwelling structures beneath the supercontinent interior varies with lithosphere thickness and viscosity. Where slabs impinge on the top of an evolving plume head (when continental and cratonic lithosphere are thick and viscous in our simulations), the cold slabs can reduce the magnitude of an evolving plume. Conversely, when the continental lithosphere is thin and weak in our simulations, slab dips shallow in the upper mantle and descend adjacent to the evolving plume, sweeping it laterally near the core-mantle boundary. These contrasting evolutions alter the magnitude of the thermal anomaly and the degree to which the plume can thin the lithosphere prior to breakup.

Plain Language Summary Tectonic plates have gone through many cycles throughout geological history with continents colliding to form supercontinents and then breaking apart to reassemble elsewhere. The way in which Earth's surface and interior work together to drive this process is not well understood. We consider the relationship between slabs, which sink toward the core-mantle boundary (CMB) as a supercontinent assembles, and plumes, which rise from the CMB to the surface and may aid in supercontinent breakup. We find that the structure of Earth's surface layer can change the morphology of slabs as they descend. This is important as slabs may determine the location and magnitude of plumes in the deep Earth, depending on the way that slabs and plumes interact. These plumes may feed back toward supercontinent breakup as they thin the Earth's surface layer, the lithosphere, indicating that the dynamics at the surface during the formation of the supercontinent may affect the forces contributing to breakup.

1. Introduction

Supercontinent cycles represent one of the largest spatial and temporal processes on Earth, with each supercontinent breaking up and reassembling over hundreds of millions of years. This cycle has important implications on climatic and biological systems through time (Nance et al., 2014; Santosh, 2010) and represents the interaction of countless Earth processes. From plate tectonics to hot-spot volcanism, many of the geological features and processes that we observe today are the result of the interaction between the mantle and lithosphere through the supercontinent cycle. Despite this, the degree of feedback between these two domains remains poorly constrained, largely due to the complexity of Earth systems and the lack of accessible primary data from the mantle.

The processes which drive supercontinent breakup have long been discussed, with two end members often being the focus; subduction at the edges of the supercontinent (slab pull or slab suction (Conrad & Lithgow-Bertelloni, 2002, 2004)) and plumes rising beneath the continental landmass to drive breakup from the interior (plume push (Dang et al., 2024; Zhang et al., 2018)). The processes, and the evolution of our understanding regarding supercontinent cycles are summarized in reviews by Chen et al. (2020), Mitchell et al. (2021), and Nance et al. (2014). Previous studies have suggested a close relationship between the two end member processes

Validation: A. Plimmer, J. H. Davies
Visualization: A. Plimmer
Writing – original draft: A. Plimmer
Writing – review & editing: A. Plimmer, J. H. Davies, J. Panton

(Anderson, 1982; Heron et al., 2015; Z.-X. Li & Zhong, 2009; Santosh et al., 2009; Wolstencroft & Davies, 2017; Yoshida & Santosh, 2011), though the degree to which upwellings and downwellings are coupled in the mantle is debated (Condie et al., 2015; Heron & Lowman, 2011). Gurnis (1988) presented a 2D rectangle model in which a supercontinent dispersed in response to mantle flow and indicated a strong relationship between the supercontinent and long-wavelength thermal structures. Since then, numerous models have attempted to constrain the relationship between mantle structures and the lithosphere in both 2D and 3D geometries (e.g., Heron & Lowman, 2011; Heron et al., 2015; Phillips & Bunge, 2007; Yoshida & Santosh, 2011; Zahirovic et al., 2015; Zhang et al., 2009). The lithosphere is often simplified to a viscous homogeneous layer (Becker & O'Connell, 2001; Jian et al., 2022), where viscous continental "caps" are implemented at the model surface (Coltice et al., 2009; Phillips & Bunge, 2007; Zhang et al., 2009), or models are initiated from a static, hypothetical supercontinent of uniform thickness (Yoshida, 2010, 2013). Zahirovic et al. (2015) showed that plate velocities are related to the proportion of continental and cratonic lithosphere, indicating the importance of such differentiation in understanding mantle driving forces. Dang et al. (2020, 2024) distinguished cratonic, orogenic, and oceanic lithosphere, where each domain is assigned a thickness and yield stress within 3D spherical simulations, constrained by free-slip boundary conditions at the surface. We build upon this approach, differentiating between oceanic, continental, and cratonic lithospheres that are consistent with a published plate motion history, implemented as a boundary condition in our 3D spherical mantle circulation models.

We aim to evaluate the role of lithosphere heterogeneity throughout the supercontinent cycle. We break this down into four phases within the mantle; the effect of lithosphere thickness and viscosity on slab dip and sinking trajectory, proximity of slabs and plumes beneath a supercontinent interior in response to the varying slab dips, the effect of slab-plume proximity on the magnitude of upwellings beneath a supercontinent interior, and the ability of these upwellings to significantly thin the thermal lithosphere. Ultimately, we aim to investigate the way in which lithosphere structure (with varying lithosphere thicknesses and viscosities) can affect mantle dynamics throughout the supercontinent cycle from assembly toward breakup.

2. Methods

2.1. Modeling Method

Modeling was carried out using the 3D mantle convection code, TERRA (Baumgardner, 1985; Bunge & Baumgardner, 1995; Bunge et al., 1997; Davies et al., 2013; Yang & Baumgardner, 2000). We assume incompressibility (McKenzie et al., 1974) and apply the Boussinesq approximation to give the equations for conservation of mass (Equation 1), energy (Equation 2), and momentum (Equation 3):

$$\nabla \cdot \boldsymbol{u} = 0 \tag{1}$$

$$\frac{\partial T}{\partial t} + \boldsymbol{u} \cdot \nabla T - \kappa \nabla^2 T - \frac{H}{C_p} = 0 \tag{2}$$

$$\nabla \cdot \left(\mu\left\{\nabla \boldsymbol{u} + (\nabla \boldsymbol{u})^T\right\}\right) - \nabla P + \alpha\rho(T_{av} - T)\, g = 0 \tag{3}$$

where u is fluid velocity, ρ is density, C_p the specific heat at constant pressure, T the temperature field, t is time, κ the thermal diffusivity, H the radiogenic heat production, μ the dynamic viscosity, P the dynamic pressure field, α is the thermal expansivity, T_{av} is the average mantle temperature, and g the gravitational acceleration.

Calculations are performed on a structured regular mesh based on an icosahedron (Baumgardner & Frederickson, 1985), with over 10 million grid points and an average radial spacing of 45 km, extending from the model Earth's surface to the core-mantle boundary (CMB) across 65 radial layers. At the CMB, the lateral spacing is approximately 32.7 km, increasing to 59.9 km at the model surface. Each simulation is analyzed from 460 Ma to present to allow for the assembly and dispersal of supercontinent Pangea, following a conditioning period. Simulations are initiated from a randomly perturbed temperature field, with a two-layer (upper and lower mantle) viscosity structure, with no viscous lithosphere, and a free-slip boundary condition at the surface and CMB to allow this initial field to evolve and develop mantle upwellings and downwellings. At this stage, the mantle flow patterns are not spatially consistent with the plate motion reconstruction at the beginning of our investigation. Therefore we apply the plate motion reconstruction of Müller et al. (2022) as a surface boundary condition, accompanied by a

Table 1
Model Parameters

Parameter	Symbol	Value	Units
Reference density	ρ	4,500	kg m^{-3}
Gravitational acceleration	g	10	m s^{-2}
Thermal expansivity	α	2.5×10^{-5}	K^{-1}
Thermal diffusivity	k	9×10^{-6}	m^2 s^{-1}
Specific heat capacity	C_p	1,000	J K^{-1} kg^{-1}
Radiogenic heat production rate	H	4.0×10^{-12}	W kg^{-1}
Surface temperature	T_s	300	K
CMB temperature	T_{CMB}	3,000	K
Reference viscosity	μ	1.0×10^{22}	Pa s
Rayleigh number	Ra	$\approx 10^7$	–

change to a 3-layer viscosity structure where the lithosphere is a factor of 100 more viscous than the reference viscosity (μ) down to 90 km depth, and then decreases to the reference value, before increasing to a value 30 times greater than the reference in the lower mantle. This phase of conditioning is run from 500 to 460 Ma, so that the mantle flow field is consistent with the plate motion history for the beginning of our circulation simulations.

The chosen plate motion model comprises a global set of topological plate polygons with associated plate boundaries and velocities at 1 Myr intervals. Briefly, this model is based on a "mantle reference frame" where plate positions are estimated relative to the mantle through time. The convecting mantle is not a stable reference frame, therefore this method minimizes net lithospheric rotation and expresses plate motion as rotations relative to a stationary axis. This model combines the plate motion model of Merdith et al. (2021), and the tectonic-rules-based approach to mantle reference frames proposed by Tetley et al. (2019). Circulation models are complex as the imposed surface velocities are set independently of the convective vigor of the mantle. Given the numerical complexity of large lateral viscosity variations at the surface, we implement a greater reference viscosity than is Earth-like to maintain computational stability and so, convection is more sluggish than what we think of the present-day mantle (Rayleigh number of 10^7 in our simulations compared to $10^8 - 10^9$ for Earth). When convection is sluggish, plate velocities must be slowed to match the natural velocity of the convective solution (Bunge et al., 2002). A scaling factor (S_v) is applied to the models according to the root mean square (RMS) velocity of the Earth surface at the present day and those calculated in convection simulations (Equation 4).

$$S_v = \frac{v_{EARTH}}{v_{MODEL}} \tag{4}$$

The present day surface RMS velocity is chosen as a representative value as the Rayleigh number of our simulations do not vary significantly, such that a constant scaling factor is preferred and the present day velocity is the best constrained. Surface velocities are multiplied by the reciprocal of S_v, ensuring that the relative plate motions are consistent with the plate motion history, just slowed to match the convective vigor of the simulations and limit surface shearing. As such, the duration of the simulation must be increased by the same factor to compensate for the reduced velocities and reflect Earth-like subduction and upwelling fluxes. Subsequently, there is an important distinction between model time (simply the assigned duration of each simulation) and Earth time (the geological time represented by the simulation). Model time is, in most cases, a factor of S_v greater than the Earth time it represents. For these simulations $S_v = 5$. For simplicity, time mentioned hereafter will refer to the equivalent Earth time.

The relevant model parameters for each of our simulations are listed in Table 1.

2.2. Identifying Different Lithospheric Domains

We utilize GPlates software (Müller et al., 2018) to produce plate velocity files compatible with TERRA. Additionally, we output files (shapefiles) which store the geometries of continents and cratons at each time step. We do not require the geometry of the oceans since it will be ascribed the default lithosphere parameters across each simulation, with a thickness of 90 km, approximating thermal oceanic lithospheres (Afonso et al., 2007; Doin & Fleitout, 1996; Walcott, 1970), and a viscosity which is two orders of magnitude greater than the upper mantle (Steinberger & Calderwood, 2006). We consider the cratons and continents as defined in the Müller et al. (2022) plate polygons and its constituent plate reconstruction model. A point-in-polygon algorithm is applied between the numerical grid points and the shapefiles. When a grid point falls within a continental or cratonic polygon, it is assigned a value of 1, or 2 respectively (Figure 1). These values are appended to the GPlates velocity files which are subsequently read into TERRA to constrain the surface boundary layer in circulation models.

Viscosity is first calculated at each node within the simulation, according to the prescribed radial profile, then altered by a given factor for continental and cratonic regions. For cratons, these factors vary between 10 and 100

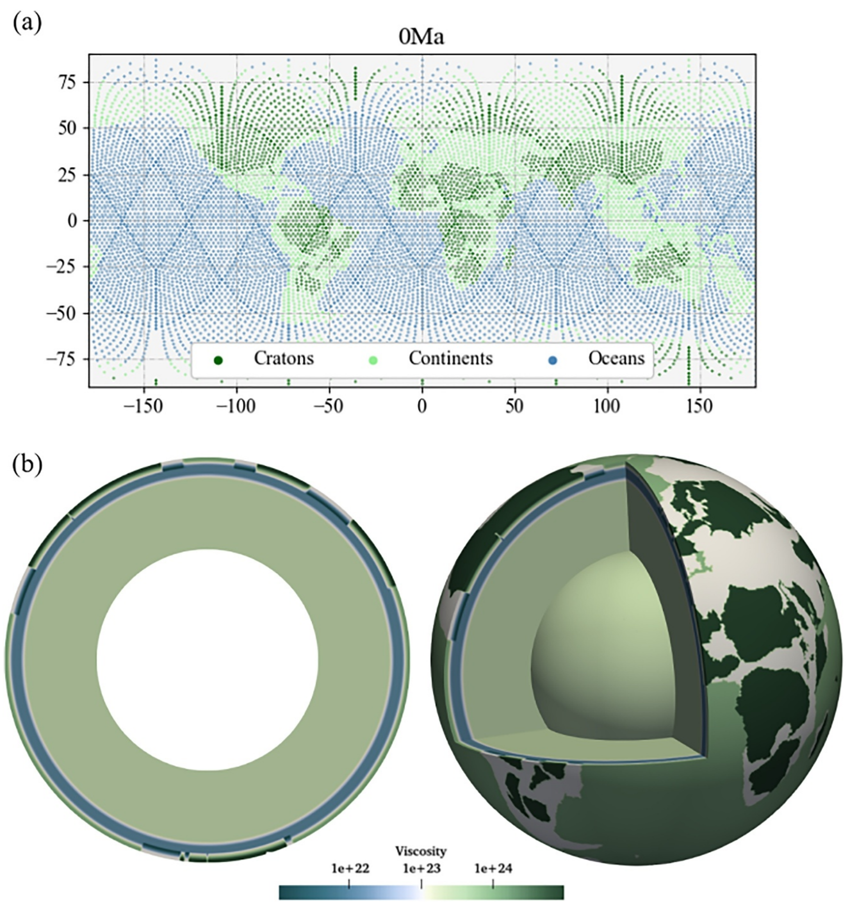

Figure 1. (a) Distribution of oceans, continents, and cratons when Time = 0 Ma expressed on the TERRA grid at a lower surface resolution of 240 km; (b) Example cross-section and 3D visualization of viscosity field when oceans, continents, and cratons have thickness of 90, 180, and 270 km, respectively, and viscosity factors of 1, 0.1, and 10 times the reference, respectively at a radial resolution of 180 km.

to reflect the highly viscous nature of stable cratonic roots (e.g., Cooper & Conrad, 2009; Lenardic & Moresi, 1999; Paul et al., 2019; Pearson et al., 2021). For continents the values vary between 0.1 and 10 to reflect the debate surrounding the relative strengths of oceanic and continental lithosphere (Carlson et al., 2005; Molnar, 1988; Pearson et al., 2021). Such an implementation supports depth, temperature and/or compositionally dependent viscosity profiles.

2.3. Parameter Space

To understand the role of different lithosphere properties, we vary the viscosity and depth of the different domains from a reference case. Each simulation is initiated in line with the parameters outlined in Table 1. We systematically vary additional parameters according to Table 2, such that each model can be compared to our reference simulation, with a homogeneous lithosphere (case000; viscosity = $1\text{x}10^{24}$ Pa s, thickness = 90 km). In addition to the 12 simulations with depth-dependent viscosities, we also present case000_td, which is similar to our reference case except that it implements a temperature dependent viscosity according to the equation:

$$\mu = \mu_{ir} \cdot e^{(Va \cdot z' - Ea \cdot T')} \tag{5}$$

where μ_{ir} is the reference radial viscosity, Va is the non-dimensionalized constant for activation volume, z' is the non-dimensionalized depth (scaled by mantle depth), Ea is the non-dimensionalized constant for activation energy, and T' is the non-dimensionalized temperature (scaled by the temperature difference between the CMB and surface temperature). For case000_td we use $Va = 1$ and $Ea = 1.5$, representing a mild temperature dependence.

10.1029/2024GC011688

Table 2
Parameter Space

	Thickness (km)		Viscosity (Pa s)	
Model no.	Continent	Craton	Continent	Craton
000	90	90	1×10^{24}	1×10^{24}
001	90	90	1×10^{25}	1×10^{25}
002	90	90	1×10^{25}	1×10^{26}
003	90	90	1×10^{23}	1×10^{25}
004	180	180	1×10^{24}	1×10^{24}
005	180	180	1×10^{25}	1×10^{25}
006	180	180	1×10^{25}	1×10^{26}
007	180	180	1×10^{23}	1×10^{25}
008	180	270	1×10^{24}	1×10^{24}
009	180	270	1×10^{25}	1×10^{25}
010	180	270	1×10^{25}	1×10^{26}
011	180	270	1×10^{23}	1×10^{25}
000_td	90	90	2.5×10^{24}	2.5×10^{24}

To make the viscosity profile of this simulation comparable to our other simulations in the upper mantle, we increase the reference viscosity of this simulation from 1×10^{22}Pa s to 2.5×10^{22} Pa s (Figure 2). As with model 000, the lithosphere in this simulation is 100 times more viscous than the reference viscosity.

We focus primarily on simulations with a depth-dependent viscosity for a number of reasons. A temperature and depth dependent viscosity structure is less numerically stable when large lateral viscosity contrasts are implemented for the lithosphere, and uses almost 6× the computational resource. We suggest that this additional time and resource would be justifiable if the results of the simulations were significantly different however, the large lateral viscosity variation implemented through the varying lithospheres have a larger impact on the dynamics of the interior than the comparatively smaller viscosity variations attributable to temperature dependence. Nonetheless we present case000_td which includes the effects of mild temperature dependence of viscosity on our reference model.

3. Results

3.1. Effect of Lithosphere Structure on Slab Dip and Trajectory in Global 3D Simulations

Pangea formed by the collision of Laurentia and Gondwana, and the closure of the interior Rheic Ocean, therefore our results focus on the features associated with this subduction zone (Figure 3). Across the suite of simulations, oceanic lithosphere is dealt with in the same way, with a viscosity of

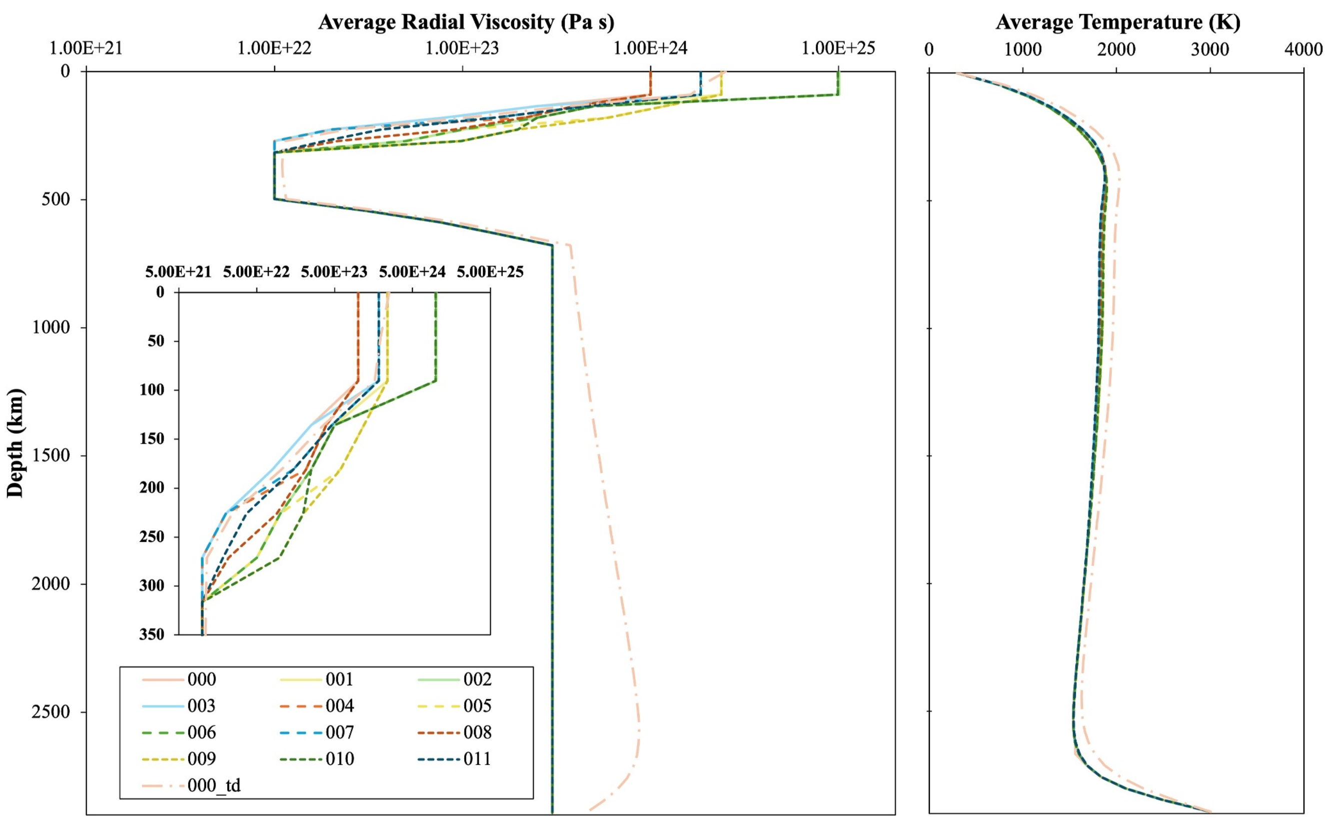

Figure 2. Average radial viscosity and temperature profiles at the end of each simulation. Inset: Average radial viscosity profiles, focusing on the uppermost 350 km.

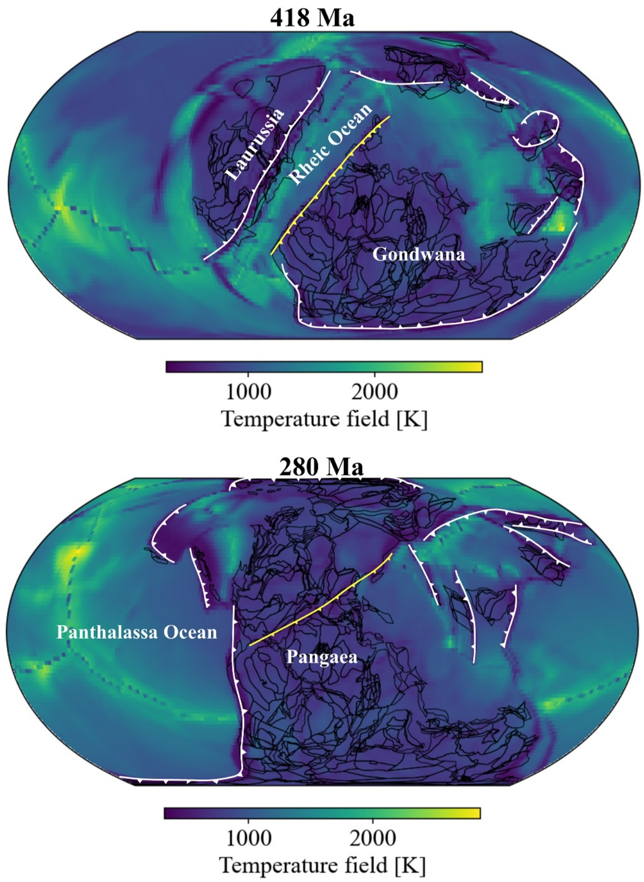

Figure 3. Temperature field of reference model at 415 Ma and 280 Ma, at 90 km depth. Subduction zones are shown by white lines. Subduction zone highlighted in yellow demarcates the focus of this study (Rheic suture). At 280 Ma, this subduction zone is no longer active but the associated cold temperature anomaly is visible beneath Pangea.

10^{24} Pa s, and a thickness of 90 km. Therefore, the differences across the models can be attributed to the thickness and viscosities of the continental and cratonic lithosphere as the supercontinent assembles.

In each simulation, the interior slab (which we subsequently refer to as slab A; defined by a −350°K temperature anomaly) detaches from the lithosphere at the surface at 335 Ma. To understand the implications of lithosphere heterogeneity on slab behavior, we therefore focus on the period of slab evolution prior to this time. The slabs can be grouped into four broad geometries, based on lateral extent at the surface, and subduction angle (Figure 4), measured from a −500°K temperature anomaly, to focus on the "core" of the subducting slab and ignore the surrounding mantle cooled by the slab. For cases with a lateral increase in viscosity (cases 001, 002, 005, 006, 009, 010) between the oceanic and supercontinental lithosphere (comprising continental and cratonic lithosphere) we find limited lateral trajectory of the slabs relative to cases 000, 003, 007, and 011, where there is a viscosity decrease from oceanic to continental lithosphere. We find that slab morphologies vary between the reference case (000) and a similar case which includes temperature dependent viscosity (000_td; Figure 4), with the latter behaving more similarly to cases 005 and 009. We attribute this to the similarity in average surface viscosity (Figure 2) between these simulations, highlighting the importance of surface viscosity in determining slab dynamics in the upper mantle.

We suggest that the rigidity of the viscous supercontinent forces the subducting slab downwards without requiring significant lithospheric thicknesses as the velocities converge at the surface. When the supercontinent is less viscous, or as viscous as the oceanic lithosphere, the slab can instead migrate laterally until it becomes sufficiently negatively buoyant to sink further. This is especially true when the continental lithosphere is thin, in which case slab A subducts shallowly beneath the weak continent and then descends vertically as it approaches the discontinuity with the more viscous cratonic lithosphere (Figure 5, models 000,008). When the continental and cratonic lithosphere are thicker than the oceanic lithosphere, the effect of the viscous continental lithosphere is more marked, causing the slabs to sink with a consistent, near vertical trajectory.

3.2. Proximity of Slabs and Plumes in Response to Varying Lithosphere Structure

At 280 Ma, around peak supercontinent assembly, we highlight four downwelling slabs which are similar across the simulations (Figure 5). Each of these downwellings exhibit a different dynamic behavior, where slab A is detached from the lithosphere at the surface, slab B extends from the surface to near the CMB, folding in the lower mantle. Slab C thickens significantly as it passes through the transition zone near 660 km depth and develops a cold plume head as it approaches cold material already residing in the lowermost mantle whilst slab D exhibits a similar cold plume head morphology without significant thickening through the transition zone, highlighting the range of dynamic behaviors. We label the upwellings (Figure 5) beneath the supercontinent as (a) (developed beneath Laurentia), (b) (developed beneath Gondwana), and (c) (developed beneath Pangea and not ubiquitous across the simulations).

Across the suite of models, there is a notable correlation between the lithosphere viscosity structure and the nature of the interaction between slab A and upwelling iii (Figure 5). In each of our simulations, the largest continents are bound by subduction zones which sweep upwelling material toward their interior. As Pangea formed by the collision of Laurentia and Gondwana, and the closure of the interior Rheic Ocean, slab A (which we attribute to the closure of the ocean) subducts directly above the evolving upwelling iii. In our viscous models (Figure 5, models 001,002,005,006,009,010), where the cratonic and continental lithosphere are 1–2 orders of magnitude more viscous than the oceanic lithosphere, lateral slab migration is reduced compared to the less viscous cases in

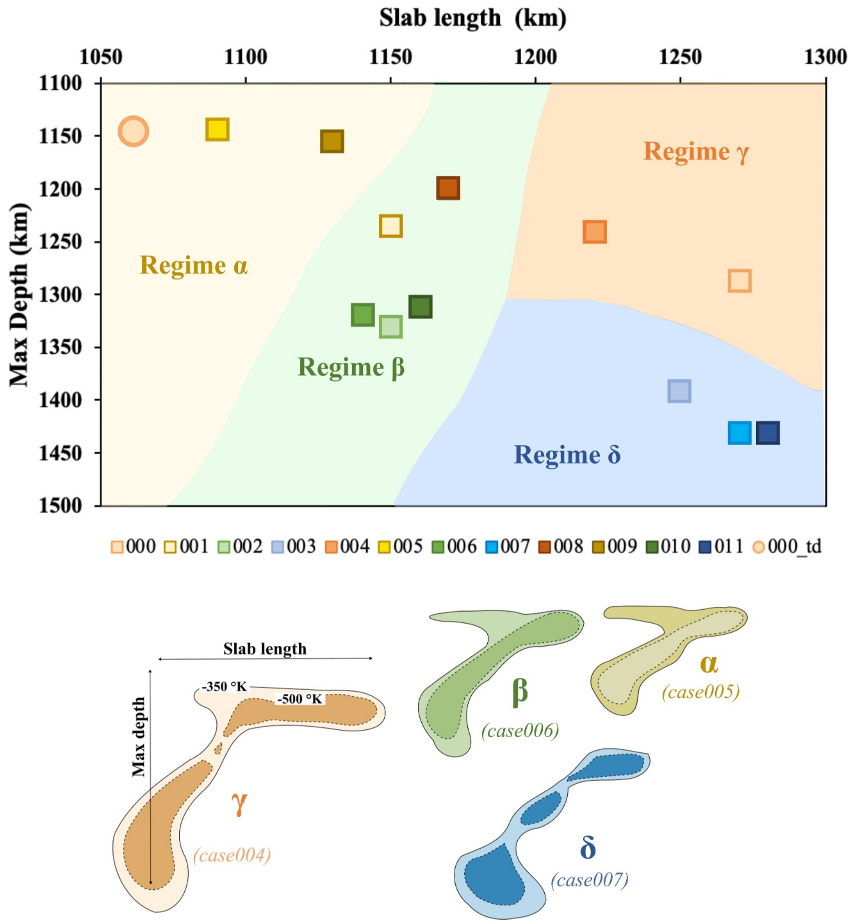

Figure 4. Comparison of slab length against depth for each simulation at 335 Ma, prior to slab break off, based on a temperature anomaly of −500°K. Models are grouped into 4 regimes based on slab geometry, labeled regime $\alpha, \beta, \gamma, \delta$. These correspond to slab geometries below. Solid black line marks the extent of the slab defined by a −350°K anomaly, while dashed line marks the extent defined by a −500°K anomaly as they appear in cross-section through the center of the subduction zone.

the uppermost mantle (Figure 4; regimes α-β), sinking directly on top of the developing upwelling, dampening out the thermal anomaly (see Movie S1 for video file). We observe that case000_td behaves similarly to other simulations classified by regime α (Figure 4, case005, case009), given the similarity in average lithosphere viscosity (Figure 2). Conversely, in the models with less viscous continents (Figure 5, models 003,007,011), the slabs descend adjacent to the developing upwelling as the slab first migrates laterally in the upper mantle (Figure 4; regimes γ-δ).

3.3. Evolution of Upwellings in Response to Downwelling Dynamics

Across our suite of models we find that large plumes develop beneath large continental landmasses. Our simulations begin at 460 Ma, at which stage Laurentia and Gondwana were the two largest continents. After 40 Myr, we observe two clusters of upwellings, interpreted as mantle plumes, which are consistent across each of our simulations. We find that one plume cluster develops rapidly beneath Gondwana, with an antipodal cluster developing beneath the Panthalassic Ocean (Figure 6). We find that these plumes are mobile in the mantle, yet the clusters in the deepest mantle remain antipodal through time, such that at the present day, they reside beneath the African continent and Pacific Ocean. We can spatially correlate these clusters at present-day with the positions of Large Low Shear Velocity Provinces at the base of the mantle.

We consider that the mobility of plumes both at the base of the mantle, and as they ascend to be related to subduction patterns at the surface. As cold downwellings descend from the surface, hot material is swept laterally

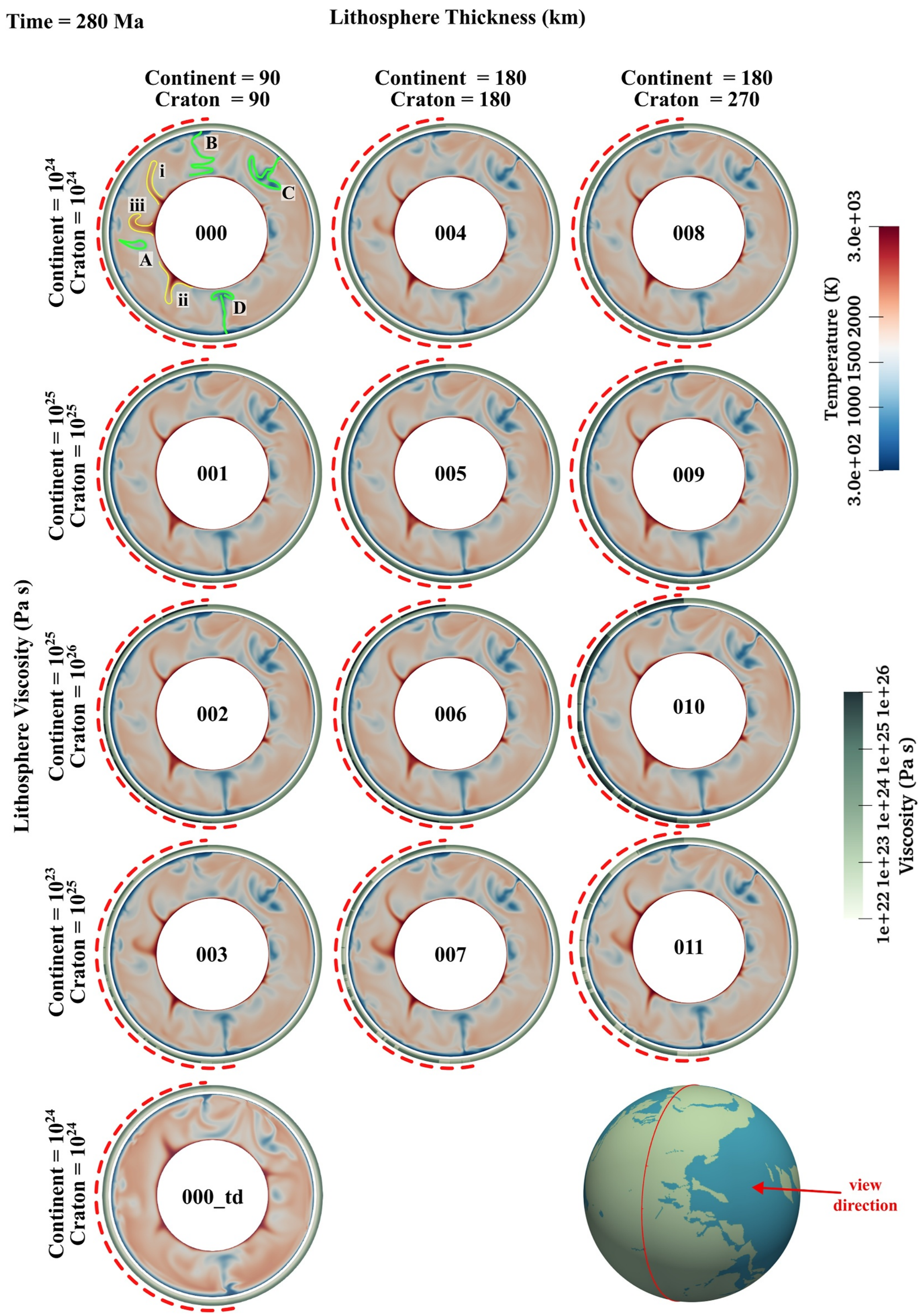

Figure 5. Slices through each simulation at 280 Ma showing the temperature field throughout the mantle and the viscosity structure from 0 to 300 km depth. Slices have been taken such that the left hemisphere comprises continental and cratonic lithosphere (dashed red line), forming the supercontinent Pangea, and the right hemisphere represents the Tethys Ocean. For case000, green lines represent the geometry of different cold downwellings, labeled A–D. Yellow lines indicate the geometry of large upwellings (i–iii). Note upwelling iii is not present across all simulations. Below is location of cross section with viewing direction.

10.1029/2024GC011688

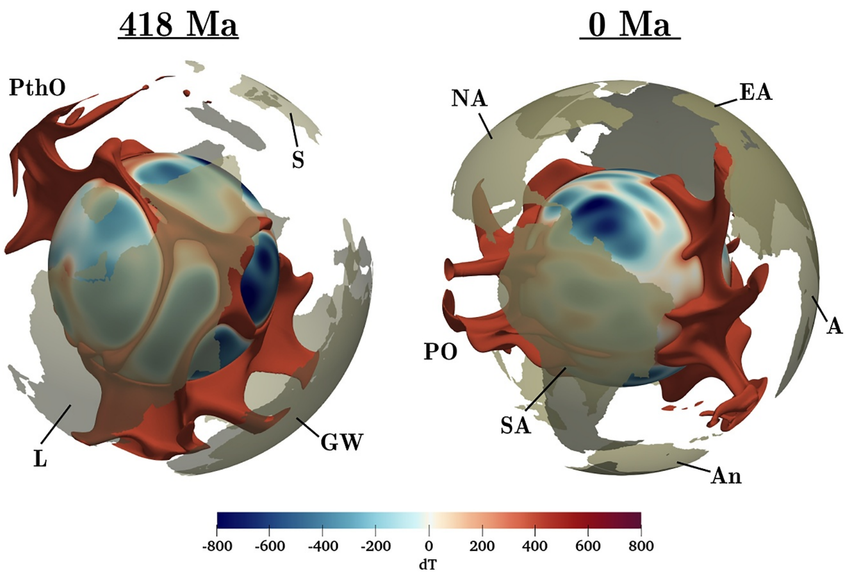

Figure 6. 3D visualization of reference case at 420 Ma, showing the clustering of plumes beneath Gondwana, and the antipodal Panthalassic Ocean. Same case at present day in our simulations, showing antipodal clusters beneath the Pacific Ocean and Africa. L, Laurentia; GW, Gondwana; PthO, Panthalassic Ocean; S, Siberia; NA, North America; SA, South America; EA, Eurasia; PO, Pacific Ocean; An, Antarctica; A, Africa. Paraview files available, see Open Research statement.

near the CMB. In fact, we consider the locations of plume development to be intrinsically linked to these downwellings. Initially, upwellings develop as broad hot regions at the CMB, but become narrow plume structures as downwelling material on either side of the upwelling sweeps the hot material toward one locus (Figure 7). Therefore, we consider that the positioning of plumes is largely determined by the clustering of hot material near the CMB induced by the return flow of slabs (also shown by Hassan et al. (2015), MacLeod et al. (2023), and Davies et al. (2012)). As supercontinents form, downflow beneath circum-continental subduction zones sweeps upwellings beneath the landmass.

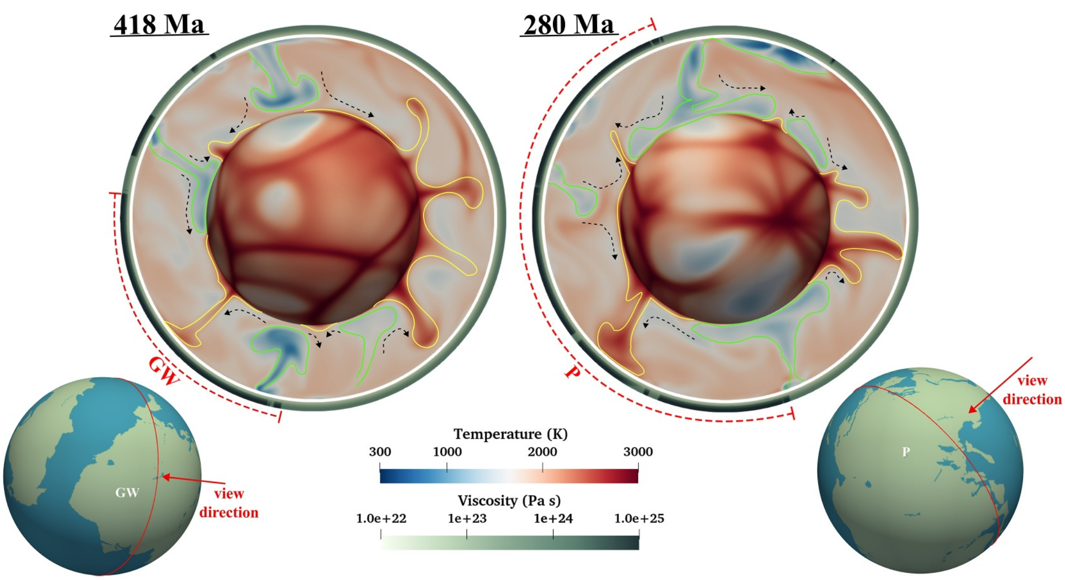

Figure 7. Slice through case005 at 418 and 280 Ma showing the interaction between downwellings slabs and mantle upwellings. Yellow lines mark the edges of hot temperature anomalies which we interpret as plumes and green lines mark the edges of cold temperature anomalies which we interpret as slabs. Black arrows indicate the flow direction induced by the downwellings, which ultimately sweeps upwelling material together into narrow plume structures. GW, Gondwana; P, Pangea. Globes indicate the corresponding cross section location and view direction.

10.1029/2024GC011688

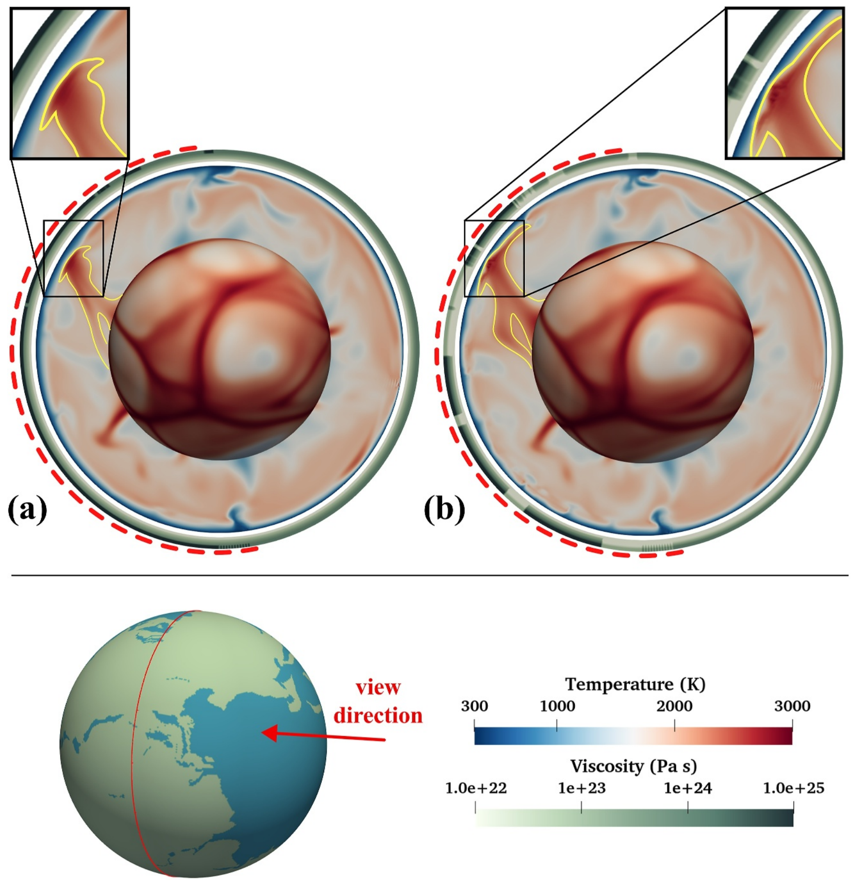

Figure 8. Evolution of the "superplume" at 177 Ma for (a) Case 001, where the slab descends on top of the upwelling (iii) and (b) Case 011, where the slab descends adjacent to the upwelling and instead sweeps the material toward upwelling (i). Yellow line encompasses the edge of the superplume and highlights the contrasting morphologies and extent of spreading beneath the lithosphere across the simulations. Insets highlight the thinning of the thermal lithosphere. Red dashed line reflects the location of the supercontinent. Below, globe view shows position of cross section with view direction.

Our simulations show that when the plumes and downwellings develop adjacent to one another beneath the supercontinent, the upwelling material is swept toward upwelling i, which is continually swept beneath the supercontinent by slab B. These upwellings merge into a strong "superplume" structure before 177 Ma, coeval with the breakup of the supercontinent Pangea (Figure 8). When the downwelling encroaches on top of the plume and reduces the magnitude of upwelling iii, upwelling i still develops into a large plume as it migrates but the magnitude is significantly smaller than in the former case. The larger superplume is sufficient to reach shallow depths and thin the thermal lithosphere whilst the extent of the smaller plume is limited and the degree of lithosphere thinning is reduced (Figure 8). These results more broadly suggest the closely coupled nature of upwelling and downwelling processes across the supercontinent cycle and the importance of lithosphere heterogeneity in sub-continental dynamics.

4. Discussion

4.1. Following the Effects of Lithosphere Heterogeneity Throughout the Supercontinent Cycle

We find that lithosphere thickness and viscosity are two factors which can alter slab dip, and trajectory through the mantle and therefore alter the proximity of subcontinental plumes and interior slabs. The interplay between these two structures have implications for the evolution of the thermal lithosphere. Where slabs (planar structures) and plumes (cylindrical structures) interact directly, the magnitude of sub-continental upwellings are limited, whilst when slabs and plumes evolve adjacent to one another, upwellings are swept toward each other, forming larger plume structures. It can be expected that large plumes are capable of significantly thinning and weakening the

10.1029/2024GC011688

lithosphere whilst smaller plumes have little effect on the thermal lithosphere. In our models, breakup will occur as dictated by the plate motion history, though we might suggest that increased lithosphere thinning would relate to an increased role for plume push in breaking supercontinents.

Our models have demonstrated the close relationship between slabs in the mantle and plume evolution. Previous studies have shown that plumes develop beneath supercontinents (e.g., Anderson, 1982; Heron & Lowman, 2011; Heron et al., 2015; Z.-X. Li & Zhong, 2009; Santosh et al., 2009; Yoshida & Santosh, 2011), though Condie et al. (2015) suggests that plume generation occurs independently of the supercontinent cycle, in response to lower mantle thermochemical dynamics. Our work is consistent with that of Heron and Lowman (2011), who showed using 3D models that subcontinental plumes develop in response to subduction patterns. We find that any large continental landmass which is bound by subduction zones, develops subcontinental plumes as hot material is swept by descending slabs. These patterns are consistent across our models, regardless of lithosphere structure, in response to the plate motion history at the surface and the associated location of subduction zones.

Across this suite of models we find that a young plume (upwelling iii) evolves beneath the center of Pangea, but the lifespan of this plume varies significantly depending on its proximity to a descending slab. We suggest that since Pangea formed through the closure of the interior Rheic Ocean, and therefore had an interior subduction zone as Gondwana and Laurentia collided, the developing plume and subducting slab evolved contemporaneously. We therefore suggest that plume development beneath a supercontinent can be intrinsically tied to subduction patterns (Heron & Lowman, 2011; Heron et al., 2015; Heyn et al., 2020), both in terms of plumes evolving in response to return flow from sinking slabs and, in the case of supercontinent introversion (where continents collide as an interior ocean closes (Martin et al., 2024; Santosh, 2010)), possible plume dampening as the slabs and plumes come into direct contact. Since the internal dynamics of the Earth and surface rheology are not well understood, we cannot determine which of our simulations is most Earth-like. Similarly, there is little geological or geophysical evidence for the deep mantle dynamics during the lifespan of Pangea. However, many studies have shown slab-plumes interactions at various mantle depths in the present day using seismic tomography (L. Li et al., 2019; Obrebski et al., 2010; Tan et al., 2002). In Figure 6 we show that the cluster of plumes beneath Pangea is similar to that currently beneath Africa. Chang et al. (2020) used seismic data and geodynamic experiments to show that the present-day Afar plume may be detached from the CMB by interaction with the Tethyan slab in the deep mantle. Therefore, whilst we cannot use our models to predict the dynamics beneath Pangea, we can suggest that the range of dynamics observed across our simulations have been observed in the present day.

Therefore, we propose that the structure of the lithosphere has the capacity to feed back into a mantle circulation cycle which ultimately determines the relative contribution of plume push forces in the breakup of a supercontinent. The viscosity structure of the supercontinent under which a slab subducts may alter the trajectory of the slab in the upper mantle and therefore alter the proximity of the slab and an evolving upwelling near the CMB. Furthermore, we find that the viscosity of the surface is more important for the behavior of slabs as they descend than the degree of temperature-dependence in mantle viscosities. Case000_td is most similar in its dynamics to cases001,005, and 009 despite the differing viscosities in the lower mantle. It is the similarity in the viscosities at the surface which determine the slab trajectory. The interaction between the interior slab and upwelling iii are also similar between these simulations (Figure 5), highlighting that the large variations in surface viscosity are more important for the dynamics of these simulations than the smaller variations in viscosity attributable to temperature-dependence. Across our models, slabs either dampen the upwelling or sweep it toward a larger developing plume. It is then the magnitude of this large plume, and its ability to thin the lithosphere which determines the role of plume push in supercontinent breakup.

We suggest that the interaction between subcontinental plumes and interior slabs will be important for any supercontinent which formed through the closure of an interior ocean (introversion). Martin et al. (2024) indicate that all previous supercontinents, except for Neoproterozoic supercontinent Rodinia, formed through introversion and therefore we propose that the implications of slab-plume interactions on the development of a subcontinental superplume which may contribute to supercontinent breakup, are likely applicable to almost all previous supercontinents.

4.2. Limitations

Our study is limited by the complexity of the lithosphere, and the difficulty in representing this within the models. Whilst we aim to introduce more complexity than some previous mantle circulation models, our simulations still

10.1029/2024GC011688

represent an oversimplification of Earth's lithosphere, given the implementation of homogeneous continents, oceans and cratons. To simplify the computational complexity of our simulations, we consider mostly depth-dependent mantle viscosity structures, where lateral variations are applied only in the lithosphere. It is worth noting that our temperature-dependent simulation has a mild temperature dependence, and that the dynamics of the downwellings and upwellings may be different if a greater temperature dependence was applied. Whilst a temperature dependent viscosity has been shown to alter the dynamics of the reference case, the behavior is still within the range of behaviors presented within this study, and is consistent with models with similar average lithosphere viscosities. We therefore suggest that whilst implementing a temperature dependent viscosity may change the dynamics of an individual simulation, the results are consistent with our findings across other similar models in this study. With greater temperature dependence we may expect the details of our results to vary more significantly, but that is not to discount our findings as a range of possible behaviors. For this study, we suggest that it is the proximity of slabs and plumes which affect the dynamics beneath the supercontinent. Therefore, whilst the dynamics of the simulations may differ under different viscosity conditions, the range of slab behaviors, and the potential for these slabs to interact with evolving plumes, remain consistent.

Additionally, when we consider the behavior of slabs and upwellings across the whole mantle depth, we must consider the behavior of structures across the transition zone at 660 km. We define this region solely as a viscosity jump, without considering any phase changes that exist within the mantle. Therefore, it is possible that both upwellings and downwellings may experience more significant changes in their velocities than our models demonstrate as they pass through phase changes. This may impact the details of our simulations, for example, the exact timing of the interactions between upwellings and downwellings. However, we suggest that mantle structures are often long-lived, on the order of 10–100 s millions of years, therefore it is proximity between slabs and plumes that is likely more important for the conclusions of this study. The recent findings of K. Li et al. (2024) show that segmented slabs can migrate more than 1,000 km along the transition zone and this suggests that future simulations in this field may benefit from implementing more complex mantle rheologies than our current configuration. However, our results are not attempting to be reflective of the real Earth dynamics, but rather present a range of possible behaviors and therefore still provide insight into the possible effects of lithosphere viscosity and thickness on mantle dynamics.

5. Conclusions

The aim of this study was to consider the role of lithosphere heterogeneity across each phase of mantle circulation during a supercontinent cycle. This holistic approach builds on previous studies to isolate the role of lithosphere viscosity and thickness on mantle dynamics from supercontinent assembly through to breakup. Lateral viscosity and thickness variations in continental lithosphere have the ability to alter the trajectory of slabs which subduct beneath them, where viscous and thicker continental lithospheres promote steeper slab dips. We, like others (e.g., Heron & Lowman, 2011; Heron et al., 2015; Z.-X. Li et al., 2003) have found that plumes develop preferentially beneath developing supercontinents as material is swept toward the interior by slabs at the edges of continents. We suggest that slabs are a significant force in shaping the morphology of upwellings structures in the lower mantle, and by extension the morphology of structures as they ascend through the mantle (Figure 9).

The proximity between slabs and plumes have the ability to substantially alter the dynamics at the surface. Subducting slabs may dampen out the signature of evolving plumes if sinking directly above the plume head, such that the contribution of plume push to supercontinent breakup is limited. Conversely, slabs may sweep plumes toward each other where they merge and reach the base of the lithosphere with a magnitude sufficient to promote lithosphere thinning. We observe varying degrees of lithosphere thinning across our models as plumes develop heterogeneously in response to varying slab morphologies, induced by differing lithosphere properties. In our suite of simulations, thin, weak continental lithosphere descend adjacent to upwellings, sweeping them toward a larger evolving plume which in turn thin the lithosphere. This suggests that the structure of the lithosphere during supercontinent formation is one of many processes which may play a role in determining the contribution of plume push forces during the late-stage of supercontinent life.

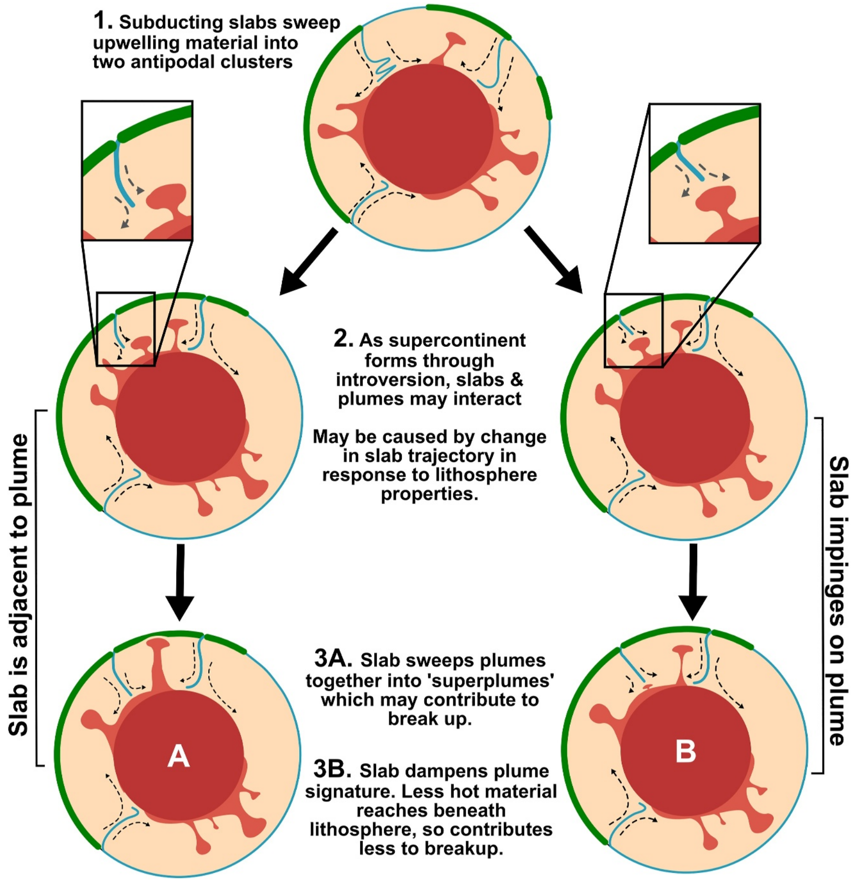

Figure 9. Schematic representation of the interactions of slabs and plumes during supercontinent assembly. Green lines represent continental lithosphere, blue lines represent oceanic lithosphere (and therefore also reflects slabs in the mantle), black arrows indicate the direction of flow around a slab. Across our suite of simulations, slabs are adjacent to plumes when the viscosity of continental lithosphere is as viscous, or less viscous than the oceanic lithosphere. Conversely, greater continental viscosities and lithosphere thicknesses promote vertical slabs, which impinge on plumes in our simulations.

Acknowledgments

This research was funded by the NERC DTP project "Constraining the relationship between mantle circulation and supercontinent cycles" (Grant NE/S007504/1), and completed alongside the work undertaken for the NERC large grant "Mantle Circulation Constrained (MC^2): A multidisciplinary 4D Earth framework for understanding mantle upwellings" (Grant NE/T012633/1) and also by the School of Earth and Environmental Sciences, Cardiff University. Numerical simulations were undertaken at (a) ARCHER2 UK National Supercomputing Service (https://www.archer2.ac.uk), and (b) HAWK, part of Supercomputing Wales, the national high-performance supercomputing system for Wales. Plate geometries and plate motion reconstructions utilized GPlates software (Müller et al., 2018) and 3D visualizations 2D slices were produced using Paraview (Ahrens et al., 2005), and map projections were produced using terratools (https://zenodo.org/records/10797186) and the Matplotlib package for Python (Hunter, 2007). This is a Cardiff CRediT Contribution 31.

Data Availability Statement

Open research results generated for this study are available at: Plimmer et al. (2024). These files contain Paraview visualization files from selected timesteps (to reduce file size) and all NetCDF files. The TERRA code used in this study predates open-source licensing. Therefore, we do not have the rights to release all parts of the code, yet segments which have been implemented for this study are available upon request. In lieu of being able to provide the source code, we provide the parameter file and compiled executable for each simulation (which differ due to the different lithospheric thicknesses which are written into the code rather than implemented through the parameter file).

References

Afonso, J., Ranalli, G., & Fernandez, M. (2007). Density structure and buoyancy of the oceanic lithosphere revisited. *Geophysical Research Letters*, *34*(10), L10302. https://doi.org/10.1029/2007GL029515

Ahrens, J., Geveci, B., & Law, C. (2005). Paraview: An end-user tool for large-data visualization. In *Visualization handbook* (pp. 717–731). https://doi.org/10.1016/B978-012387582-2/50038-1

Anderson, D. L. (1982). Hotspots, polar wander, Mesozoic convection and the geoid. *Nature*, *297*(5865), 391–393. https://doi.org/10.1038/297391a0

Baumgardner, J. R. (1985). Three-dimensional treatment of convective flow in the Earth's mantle. *Journal of Statistical Physics*, *39*(5–6), 501–511. https://doi.org/10.1007/BF01008348

Baumgardner, J. R., & Frederickson, P. O. (1985). Icosahedral discretization of the two-sphere. *SIAM Journal on Numerical Analysis*, *22*(6), 1107–1115. https://doi.org/10.1137/0722066

Becker, T. W., & O'Connell, R. J. (2001). Predicting plate velocities with mantle circulation models. *Geochemistry, Geophysics, Geosystems*, *2*(12), 1060. https://doi.org/10.1029/2001GC000171

Bunge, H.-P., & Baumgardner, J. R. (1995). Mantle convection modeling on parallel virtual machines. *Computers in Physics*, *9*(2), 207–215. https://doi.org/10.1063/1.168525
Bunge, H.-P., Richards, M. A., & Baumgardner, J. R. (1997). A sensitivity study of three-dimensional spherical mantle convection at 10^8 Rayleigh number: Effects of depth-dependent viscosity, heating mode, and an endothermic phase change. *Journal of Geophysical Research*, *102*(B6), 11991–12007. https://doi.org/10.1029/96JB03806
Bunge, H.-P., Richards, M. A., & Baumgardner, J. R. (2002). Mantle-circulation models with sequential data assimilation: Inferring present-day mantle structure from plate–motion histories. *Philosophical Transactions of the Royal Society of London,Series A: Mathematical, Physical and Engineering Sciences*, *360*(1800), 2545–2567. https://doi.org/10.1098/rsta.2002.1080
Carlson, R. W., Pearson, D. G., & James, D. E. (2005). Physical, chemical, and chronological characteristics of continental mantle. *Reviews of Geophysics*, *43*(1), RG1001. https://doi.org/10.1029/2004RG000156
Chang, S.-J., Kendall, E., Davaille, A., & Ferreira, A. M. (2020). The evolution of mantle plumes in East Africa. *Journal of Geophysical Research: Solid Earth*, *125*(12), e2020JB019929. https://doi.org/10.1029/2020jb019929
Chen, L., Wang, X., Liang, X., Wan, B., & Liu, L. (2020). Subduction tectonics vs. plume tectonics—Discussion on driving forces for plate motion. *Science China Earth Sciences*, *63*(3), 315–328. https://doi.org/10.1007/s11430-019-9538-2
Coltice, N., Bertrand, H., Rey, P., Jourdan, F., Phillips, B. R., & Ricard, Y. (2009). Global warming of the mantle beneath continents back to the Archaean. *Gondwana Research*, *15*(3–4), 254–266. https://doi.org/10.1016/j.gr.2008.10.001
Condie, K. C., Davaille, A., Aster, R. C., & Arndt, N. (2015). Upstairs-downstairs: Supercontinents and large igneous provinces, are they related? *International Geology Review*, *57*(11–12), 1341–1348. https://doi.org/10.1080/00206814.2014.963170
Conrad, C. P., & Lithgow-Bertelloni, C. (2002). How mantle slabs drive plate tectonics. *Science*, *298*(5591), 207–209. https://doi.org/10.1126/science.1074161
Conrad, C. P., & Lithgow-Bertelloni, C. (2004). The temporal evolution of plate driving forces: Importance of "slab suction" versus "slab pull" during the Cenozoic. *Journal of Geophysical Research*, *109*(B10), B10407. https://doi.org/10.1029/2004JB002991
Cooper, C., & Conrad, C. P. (2009). Does the mantle control the maximum thickness of cratons? *Lithosphere*, *1*(2), 67–72. https://doi.org/10.1130/L40.1
Dang, Z., Zhang, N., Li, Z.-X., Huang, C., Spencer, C. J., & Liu, Y. (2020). Weak orogenic lithosphere guides the pattern of plume-triggered supercontinent break-up. *Communications Earth & Environment*, *1*(1), 51. https://doi.org/10.1038/s43247-020-00052-z
Dang, Z., Zhang, N., Li, Z.-X., & Yan, P. (2024). Pangea's breakup: The roles of mantle plumes, orogens, and subduction retreat. *Geological Society, London, Special Publications*, *542*(1), 129–148. https://doi.org/10.1144/SP542-2022-345
Davies, D. R., Davies, J. H., Bollada, P. C., Hassan, O., Morgan, K., & Nithiarasu, P. (2013). A hierarchical mesh refinement technique for global 3-D spherical mantle convection modelling. *Geoscientific Model Development*, *6*(4), 1095–1107. https://doi.org/10.5194/gmd-6-1095-2013
Davies, D. R., Goes, S., Davies, J., Schuberth, B., Bunge, H.-P., & Ritsema, J. (2012). Reconciling dynamic and seismic models of Earth's lower mantle: The dominant role of thermal heterogeneity. *Earth and Planetary Science Letters*, *353–354*, 253–269. https://doi.org/10.1016/j.epsl.2012.08.016
Doin, M., & Fleitout, L. (1996). Thermal evolution of the oceanic lithosphere: An alternative view. *Earth and Planetary Science Letters*, *142*(1–2), 121–136. https://doi.org/10.1016/0012-821X(96)00082-9
Gurnis, M. (1988). Large-scale mantle convection and the aggregation and dispersal of supercontinents. *Nature*, *332*(6166), 695–699. https://doi.org/10.1038/332695a0
Hassan, R., Flament, N., Gurnis, M., Bower, D. J., & Müller, D. (2015). Provenance of plumes in global convection models. *Geochemistry, Geophysics, Geosystems*, *16*(5), 1465–1489. https://doi.org/10.1002/2015gc005751
Heron, P. J., & Lowman, J. P. (2011). The effects of supercontinent size and thermal insulation on the formation of mantle plumes. *Tectonophysics*, *510*(1–2), 28–38. https://doi.org/10.1016/j.tecto.2011.07.002
Heron, P. J., Lowman, J. P., & Stein, C. (2015). Influences on the positioning of mantle plumes following supercontinent formation. *Journal of Geophysical Research: Solid Earth*, *120*(5), 3628–3648. https://doi.org/10.1002/2014JB011727
Heyn, B. H., Conrad, C. P., & Trønnes, R. G. (2020). How thermochemical piles can (periodically) generate plumes at their edges. *Journal of Geophysical Research: Solid Earth*, *125*(6), e2019JB018726. https://doi.org/10.1029/2019JB018726
Hunter, J. D. (2007). Matplotlib: A 2D graphics environment. *Computing in Science & Engineering*, *9*(3), 90–95. https://doi.org/10.1109/MCSE.2007.55
Jian, D., Williams, S. E., Yu, S., & Zhao, G. (2022). Quantifying the link between the detrital zircon record and tectonic settings. *Journal of Geophysical Research: Solid Earth*, *127*(9), e2022JB024606. https://doi.org/10.1029/2022JB024606
Lenardic, A., & Moresi, L. (1999). Some thoughts on the stability of cratonic lithosphere: Effects of buoyancy and viscosity. *Journal of Geophysical Research*, *104*(B6), 12747–12758. https://doi.org/10.1029/1999JB900035
Li, K., Hu, J., Li, Y., Zhou, H., & Zhang, H. (2024). Slab segmentation and stacking in mantle transition zone controls disparate surface and lower mantle subducting rates and complex slab morphology. *Geophysical Research Letters*, *51*(17), e2024GL110202. https://doi.org/10.1029/2024GL110202
Li, L., Chen, Y.-W., Zheng, Y., Hu, H., & Wu, J. (2019). Seismic evidence for plume-slab interaction by high-resolution imaging of the 410-km discontinuity under Tonga. *Geophysical Research Letters*, *46*(23), 13687–13694. https://doi.org/10.1029/2019gl084164
Li, Z.-X., Li, X., Kinny, P., Wang, J., Zhang, S., & Zhou, H. (2003). Geochronology of Neoproterozoic syn-rift magmatism in the Yangtze Craton, South China and correlations with other continents: Evidence for a mantle superplume that broke up Rodinia. *Precambrian Research*, *122*(1–4), 85–109. https://doi.org/10.1016/S0301-9268(02)00208-5
Li, Z.-X., & Zhong, S. (2009). Supercontinent–superplume coupling, true polar wander and plume mobility: Plate dominance in whole-mantle tectonics. *Physics of the Earth and Planetary Interiors*, *176*(3–4), 143–156. https://doi.org/10.1016/j.pepi.2009.05.004
MacLeod, S. J., Müller, R. D., Hassan, R., & Williams, S. E. (2023). Chapter 18 - Evolution of mantle plumes and lower mantle structure in numerical models using tectonic reconstructions as boundary conditions. In J. C. Duarte (Ed.), *Dynamics of plate tectonics and mantle convection* (pp. 427–458). Elsevier. https://doi.org/10.1016/B978-0-323-85733-8.00022-6
Martin, E. L., Cawood, P. A., Murphy, J. B., Nance, R. D., & Heron, P. J. (2024). The tectonics of introversion and extroversion: Redefining interior and exterior oceans in the supercontinent cycle. *Geological Society, London, Special Publications*, *542*(1), 15–29. https://doi.org/10.1144/SP542-2023-54
McKenzie, D. P., Roberts, J. M., & Weiss, N. O. (1974). Convection in the Earth's mantle: Towards a numerical simulation. *Journal of Fluid Mechanics*, *62*(03), 465–538. https://doi.org/10.1017/S0022112074000784
Merdith, A. S., Williams, S. E., Collins, A. S., Tetley, M. G., Mulder, J. A., Blades, M. L., et al. (2021). Extending full-plate tectonic models into deep time: Linking the Neoproterozoic and the Phanerozoic. *Earth-Science Reviews*, *214*, 103477. https://doi.org/10.1016/j.earscirev.2020.103477

Mitchell, R. N., Zhang, N., Salminen, J., Liu, Y., Spencer, C. J., Steinberger, B., et al. (2021). The supercontinent cycle. *Nature Reviews Earth & Environment*, *2*(5), 358–374. https://doi.org/10.1038/s43017-021-00160-0

Molnar, P. (1988). Continental tectonics in the aftermath of plate tectonics. *Nature*, *335*(6186), 131–137. https://doi.org/10.1038/335131a0

Müller, R. D., Cannon, J., Qin, X., Watson, R. J., Gurnis, M., Williams, S., et al. (2018). GPlates: Building a virtual Earth through deep time. *Geochemistry, Geophysics, Geosystems*, *19*(7), 2243–2261. https://doi.org/10.1029/2018GC007584

Müller, R. D., Flament, N., Cannon, J., Tetley, M. G., Williams, S. E., Cao, X., et al. (2022). A tectonic-rules-based mantle reference frame since 1 billion years ago–implications for supercontinent cycles and plate–mantle system evolution. *Solid Earth*, *13*(7), 1127–1159. https://doi.org/10.5194/se-13-1127-2022

Nance, R. D., Murphy, J. B., & Santosh, M. (2014). The supercontinent cycle: A retrospective essay. *Gondwana Research*, *25*(1), 4–29. https://doi.org/10.1016/j.gr.2012.12.026

Obrebski, M., Allen, R. M., Xue, M., & Hung, S.-H. (2010). Slab-plume interaction beneath the Pacific Northwest. *Geophysical Research Letters*, *37*(14), L14305. https://doi.org/10.1029/2010gl043489

Paul, J., Ghosh, A., & Conrad, C. P. (2019). Traction and strain-rate at the base of the lithosphere: An insight into cratonic survival. *Geophysical Journal International*, *217*(2), 1024–1033. https://doi.org/10.1093/gji/ggz079

Pearson, D. G., Scott, J. M., Liu, J., Schaeffer, A., Wang, L. H., van Hunen, J., et al. (2021). Deep continental roots and cratons. *Nature*, *596*(7871), 199–210. https://doi.org/10.1038/s41586-021-03600-5

Phillips, B. R., & Bunge, H.-P. (2007). Supercontinent cycles disrupted by strong mantle plumes. *Geology*, *35*(9), 847–850. https://doi.org/10.1130/G23686A.1

Plimmer, A., Davies, J. H., & Panton, J. (2024). Mantle structures beneath an evolving supercontinent [Dataset]. *Zenodo*. https://zenodo.org/records/11128003

Santosh, M. (2010). Supercontinent tectonics and biogeochemical cycle: A matter of 'life and death'. *Geoscience Frontiers*, *1*(1), 21–30. https://doi.org/10.1016/j.gsf.2010.07.001

Santosh, M., Maruyama, S., & Yamamoto, S. (2009). The making and breaking of supercontinents: Some speculations based on superplumes, super downwelling and the role of tectosphere. *Gondwana Research*, *15*(3–4), 324–341. https://doi.org/10.1016/j.gr.2008.11.004

Steinberger, B., & Calderwood, A. R. (2006). Models of large-scale viscous flow in the Earth's mantle with constraints from mineral physics and surface observations. *Geophysical Journal International*, *167*(3), 1461–1481. https://doi.org/10.1111/j.1365-246X.2006.03131.x

Tan, E., Gurnis, M., & Han, L. (2002). Slabs in the lower mantle and their modulation of plume formation. *Geochemistry, Geophysics, Geosystems*, *3*(11), 1–24. https://doi.org/10.1029/2001gc000238

Tetley, M. G., Williams, S. E., Gurnis, M., Flament, N., & Müller, R. D. (2019). Constraining absolute plate motions since the Triassic. *Journal of Geophysical Research: Solid Earth*, *124*(7), 7231–7258. https://doi.org/10.1029/2019JB017442

Walcott, R. (1970). Flexural rigidity, thickness, and viscosity of the lithosphere. *Journal of Geophysical Research*, *75*(20), 3941–3954. https://doi.org/10.1029/JB075i020p03941

Wolstencroft, M., & Davies, J. H. (2017). Breaking supercontinents; no need to choose between passive or active. *Solid Earth*, *8*(4), 817–825. https://doi.org/10.5194/se-8-817-2017

Yang, W.-S., & Baumgardner, J. R. (2000). A matrix-dependent transfer multigrid method for strongly variable viscosity infinite Prandtl number thermal convection. *Geophysical & Astrophysical Fluid Dynamics*, *92*(3–4), 151–195. https://doi.org/10.1080/03091920008203715

Yoshida, M. (2010). Preliminary three-dimensional model of mantle convection with deformable, mobile continental lithosphere. *Earth and Planetary Science Letters*, *295*(1–2), 205–218. https://doi.org/10.1016/j.epsl.2010.04.001

Yoshida, M. (2013). Mantle temperature under drifting deformable continents during the supercontinent cycle. *Geophysical Research Letters*, *40*(4), 681–686. https://doi.org/10.1002/grl.50151

Yoshida, M., & Santosh, M. (2011). Supercontinents, mantle dynamics and plate tectonics: A perspective based on conceptual vs. numerical models. *Earth-Science Reviews*, *105*(1–2), 1–24. https://doi.org/10.1016/j.earscirev.2010.12.002

Zahirovic, S., Müller, R. D., Seton, M., & Flament, N. (2015). Tectonic speed limits from plate kinematic reconstructions. *Earth and Planetary Science Letters*, *418*, 40–52. https://doi.org/10.1016/j.epsl.2015.02.037

Zhang, N., Dang, Z., Huang, C., & Li, Z.-X. (2018). The dominant driving force for supercontinent breakup: Plume push or subduction retreat? *Geoscience Frontiers*, *9*(4), 997–1007. https://doi.org/10.1016/j.gsf.2018.01.010

Zhang, N., Zhong, S., & McNarmara, A. K. (2009). Supercontinent formation from stochastic collision and mantle convection models. *Gondwana Research*, *15*(3–4), 267–275. https://doi.org/10.1016/j.gr.2008.10.002